AMERICAN SOCIETY FOR MICROBIOLOGY | Journal of Virology®

PATHOGENESIS AND IMMUNITY

Virologic and Immunologic Features of Simian Immunodeficiency Virus Control Post-ART Interruption in Rhesus Macaques

Zachary Strongin,[a] Luca Micci,[a] Rémi Fromentin,[b,c] Justin Harper,[a] Julia McBrien,[a] Emily Ryan,[a] Neeta Shenvi,[d] Kirk Easley,[d] Nicolas Chomont,[b,c] Guido Silvestri,[a,e] Mirko Paiardini[a,e]

[a]Division of Microbiology and Immunology, Yerkes National Primate Research Center, Emory University, Atlanta, Georgia, USA
[b]Centre de recherche du CHUM, Montreal, Quebec, Canada
[c]Department of Microbiology, Infectiology and Immunology, Université de Montréal, Montreal, Quebec, Canada
[d]Rollins School of Public Health, Emory University, Atlanta, Georgia, USA
[e]Department of Pathology and Laboratory Medicine, Emory University School of Medicine, Atlanta, Georgia, USA

ABSTRACT Antiretroviral therapy (ART) cannot eradicate human immunodeficiency virus (HIV) and a rapid rebound of virus replication follows analytical treatment interruption (ATI) in the vast majority of HIV-infected individuals. Sustained control of HIV replication without ART has been documented in a subset of individuals, defined as posttreatment controllers (PTCs). The key determinants of post-ART viral control remain largely unclear. Here, we identified 7 SIV_{mac239}-infected rhesus macaques (RMs), defined as PTCs, who started ART 8 weeks postinfection, continued ART for >7 months, and controlled plasma viremia at $<10^4$ copies/ml for up to 8 months after ATI and <200 copies/ml at the latest time point. We characterized immunologic and virologic features associated with post-ART SIV control in blood, lymph node (LN), and colorectal (RB) biopsy samples compared to 15 noncontroller (NC) RMs. Before ART initiation, PTCs had higher CD4 T cell counts, lower plasma viremia, and SIV-DNA content in blood and LN compared to NCs, but had similar CD8 T cell function. While levels of intestinal CD4 T cells were similar, PTCs had higher frequencies of Th17 cells. On ART, PTCs had significantly lower levels of residual plasma viremia and SIV-DNA content in blood and tissues. After ATI, SIV-DNA content rapidly increased in NCs, while it remained stable or even decreased in PTCs. Finally, PTCs showed immunologic benefits of viral control after ATI, including higher CD4 T cell levels and reduced immune activation. Overall, lower plasma viremia, reduced cell-associated SIV-DNA, and preserved Th17 homeostasis, including at pre-ART, are the main features associated with sustained viral control after ATI in SIV-infected RMs.

IMPORTANCE While effective, antiretroviral therapy is not a cure for HIV infection. Therefore, there is great interest in achieving viral remission in the absence of antiretroviral therapy. Posttreatment controllers represent a small subset of individuals who are able to control HIV after cessation of antiretroviral therapy, but characteristics associated with these individuals have been largely limited to peripheral blood analysis. Here, we identified 7 SIV-infected rhesus macaques that mirrored the human posttreatment controller phenotype and performed immunologic and virologic analysis of blood, lymph node, and colorectal biopsy samples to further understand the characteristics that distinguish them from noncontrollers. Lower viral burden and preservation of immune homeostasis, including intestinal Th17 cells, both before and after ART, were shown to be two major factors associated with the ability to achieve posttreatment control. Overall, these results move the field further toward understanding of important characteristics of viral control in the absence of antiretroviral therapy.

Citation Strongin Z, Micci L, Fromentin R, Harper J, McBrien J, Ryan E, Shenvi N, Easley K, Chomont N, Silvestri G, Paiardini M. 2020. Virologic and immunologic features of simian immunodeficiency virus control post-ART interruption in rhesus macaques. J Virol 94:e00338-20. https://doi.org/10.1128/JVI.00338-20.

Editor Viviana Simon, Icahn School of Medicine at Mount Sinai

Copyright © 2020 American Society for Microbiology. All Rights Reserved.

Address correspondence to Mirko Paiardini, mirko.paiardini@emory.edu.

Received 26 February 2020
Accepted 17 April 2020
Accepted manuscript posted online 29 April 2020
Published 1 July 2020

KEYWORDS HIV-1, PTC, SIV, Th17, analytic treatment interruption, posttreatment controller, viral rebound

The advent of modern antiretroviral therapy (ART) has allowed for suppression of HIV-1 replication in HIV-1-infected individuals and has dramatically reduced HIV morbidity and mortality (1, 2). Unfortunately, due to the establishment of a pool of quiescent, infected CD4 T cells that harbor replication-competent virus, discontinuation of daily ART leads to rapid viral rebound and continued disease progression in most individuals (3, 4). Therefore, there is great interest in understanding the mechanisms regulating HIV persistence, the virologic and immunologic correlates of viral rebound, and the approaches that may lead to maintenance of viremic control after treatment interruption.

One model of such control is seen in a subset of patients referred to as posttreatment controllers (PTCs). These individuals, best characterized by the VISCONTI and CHAMP studies, display an ability to maintain viral suppression after undergoing analytic treatment interruption (ATI) (5, 6). While definitions vary by study, PTCs are typically characterized as maintaining plasma viral loads less than 400 copies/ml for at least 6 months following ATI (5–12). Importantly, they seem to represent a distinct group from the more widely characterized elite controller (EC) population. While ECs have been shown to have an overrepresentation of protective HLA alleles (B*27 and B*57), PTCs do not appear to be enriched in these alleles and so far have been shown to have inferior CD8 activity compared to traditional ECs (6, 13). In fact, these individuals may be more likely to carry HLA alleles previously characterized as "risk" alleles (6). Furthermore, posttreatment control is more widely observed than spontaneous control, with the occurrence estimated to range between 5 and 15% of individuals undergoing ATI, compared to the estimated EC frequency of $<$0.5% (14, 15). As most approaches targeted at achieving a functional HIV cure utilize HIV control after ATI as a primary readout, it is important to understand the dynamics of HIV control in order to target interventions toward this outcome, as well as be able to distinguish intervention-based control from naturally occurring posttreatment control.

Current studies have been unable to identify the driving mechanisms for PTCs, but control has been associated with earlier initiation of ART, lower prevalence of infected long-lived CD4 T cells (central memory), and an overall smaller reservoir size prior to cessation of treatment (5, 6, 15–17). Importantly, early initiation of ART may function to both limit the size of the reservoir as well as preserve immune function, allowing for robust immune control of the virus after treatment. Unfortunately, as with many HIV studies, characterization of PTCs has been largely limited to analyses of peripheral blood samples and limited analyses have been performed in early infection, before initiation of ART. Further challenging to a broad understanding of the dynamics of posttreatment control are the limitations of differing infection kinetics and demographics within and across cohorts of human PTCs.

The established SIV model of HIV infection using rhesus macaques (RMs) allows for longitudinal investigations into dynamics of immunologic and virologic parameters of HIV infection, including in tissues. In this study, we identified 7 SIV-infected RMs that exhibit posttreatment control, allowing us to characterize features of virologic control that further the understanding of the PTC phenomenon. Despite identical viral infection and treatment timelines as noncontroller RMs, these animals showed robust control of viremia post-ATI, with viral loads less than 10^4 copies/ml for the entire post-ATI follow-up and less than 200 copies/ml at the latest experimental point, similar to previously described human PTCs. We have identified important factors that seem to be associated with this control, including reduced SIV "exposure" prior to ART initiation, better preservation of blood and LN CD4 T cells, as well as of intestinal Th17 cells, lower levels of immune activation, and a smaller reservoir size. Although limited in size, this study enhances and expands to tissues the understanding of posttreatment control

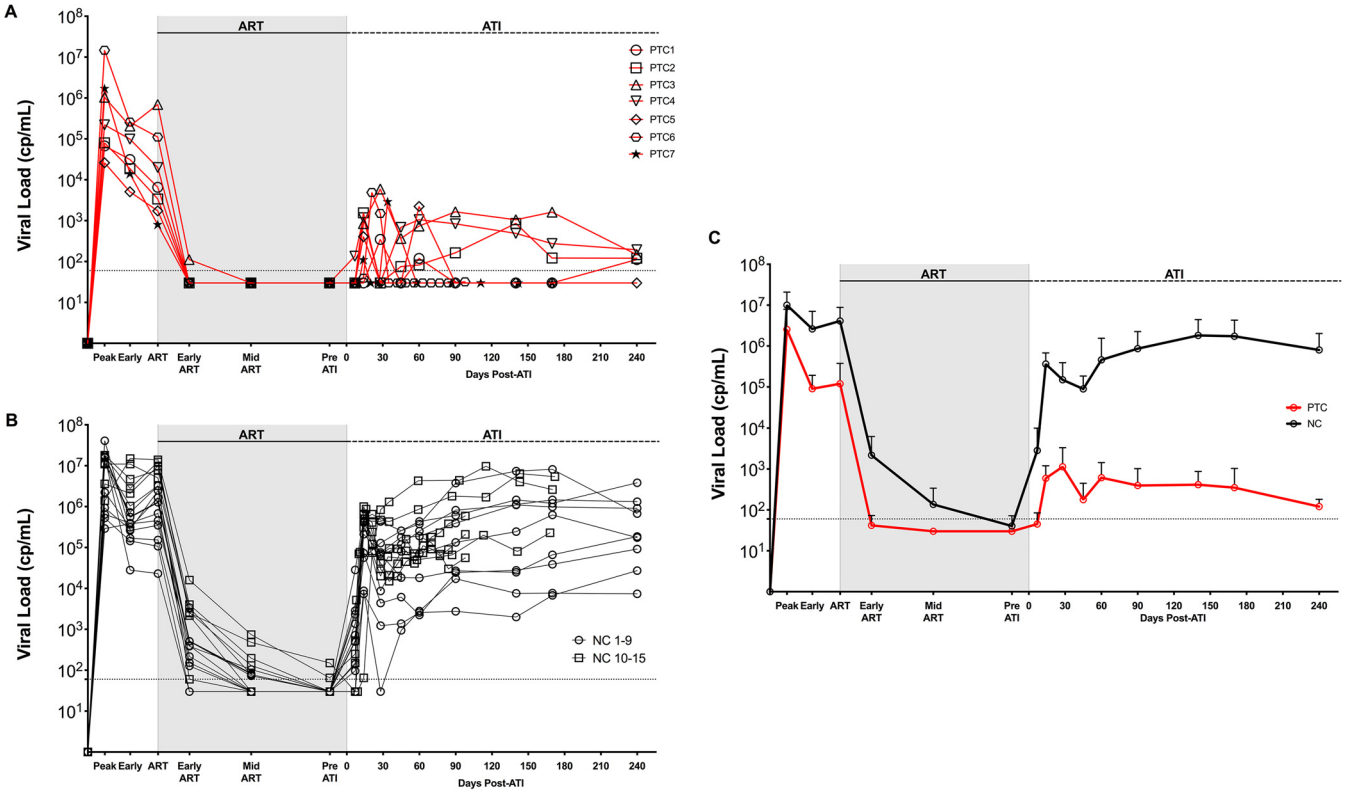

FIG 1 PTCs exhibit strong viral control after ART interruption. (A and B) Plasma viral load for PTCs (A) ($n = 7$) and NCs (B) ($n = 15$) at multiple time points throughout infection (see the Materials and Methods for definitions). NC1 to 9 are those included in all subsequent analyses. (C) Average viral load for PTCs and NCs displayed as mean ± standard deviation (SD). Shaded area designates the period for which animals were on ART. Dotted line designates the limit of detection (60 copies/ml).

and suggests that nonhuman primate models of HIV can serve as an important tool in understanding and targeting critical mechanisms of viral control in the absence of ART.

RESULTS

Identification of posttreatment controllers among SIV-infected rhesus macaques. Among different studies performed at the Yerkes National Primate Research Center in which rhesus macaques (RMs) were experimentally infected with SIV, initiated on ART, and underwent analytic treatment interruption (ATI), we identified 7 RMs with superior ability to control viral rebound after ATI compared to what is normally seen in $SIVmac_{239}$-infected RMs. Specifically, these 7 RMs, defined as posttreatment controllers (PTCs) maintained plasma viremia of $<10^4$ copies/ml up to 8 months post-interruption and all had viral loads of <200 copies/ml at the final experimental time point (Fig. 1A). To investigate the main features associated with posttreatment control, multiple virologic and immunologic parameters were assessed and compared with those of 15 RM noncontrollers (NCs) that did not control viral rebound after ATI, with plasma viremia of $>10^4$ copies/ml for the majority of posttreatment follow-up (Fig. 1B). Among the large number of $SIVmac_{239}$-infected RMs that do not control viral rebound after ATI, these 15 animals were selected because they matched the experimental conditions used for the 7 PTCs, including (i) being infected via the same route and with the same virus (intravenously; $SIVmac_{239}$); (ii) starting ART 8 weeks postinfection (p.i.); (iii) being on ART for a period between 7 to 14 months; and (iv) having multiple viral load measures following ATI, with many of those overlapping with the PTCs in terms of time post-ATI. Characteristics of each animal are described in Table S1. All 22 animals were negative for B*08 and B*17, the MHC class I alleles associated with the control of SIV replication (18, 19). Five out of 7 PTCs were $MamuA01^+$, compared to 4 out of 15 NCs. As indicated in Table S1, two different ART regimens were used, with a similar PTC and

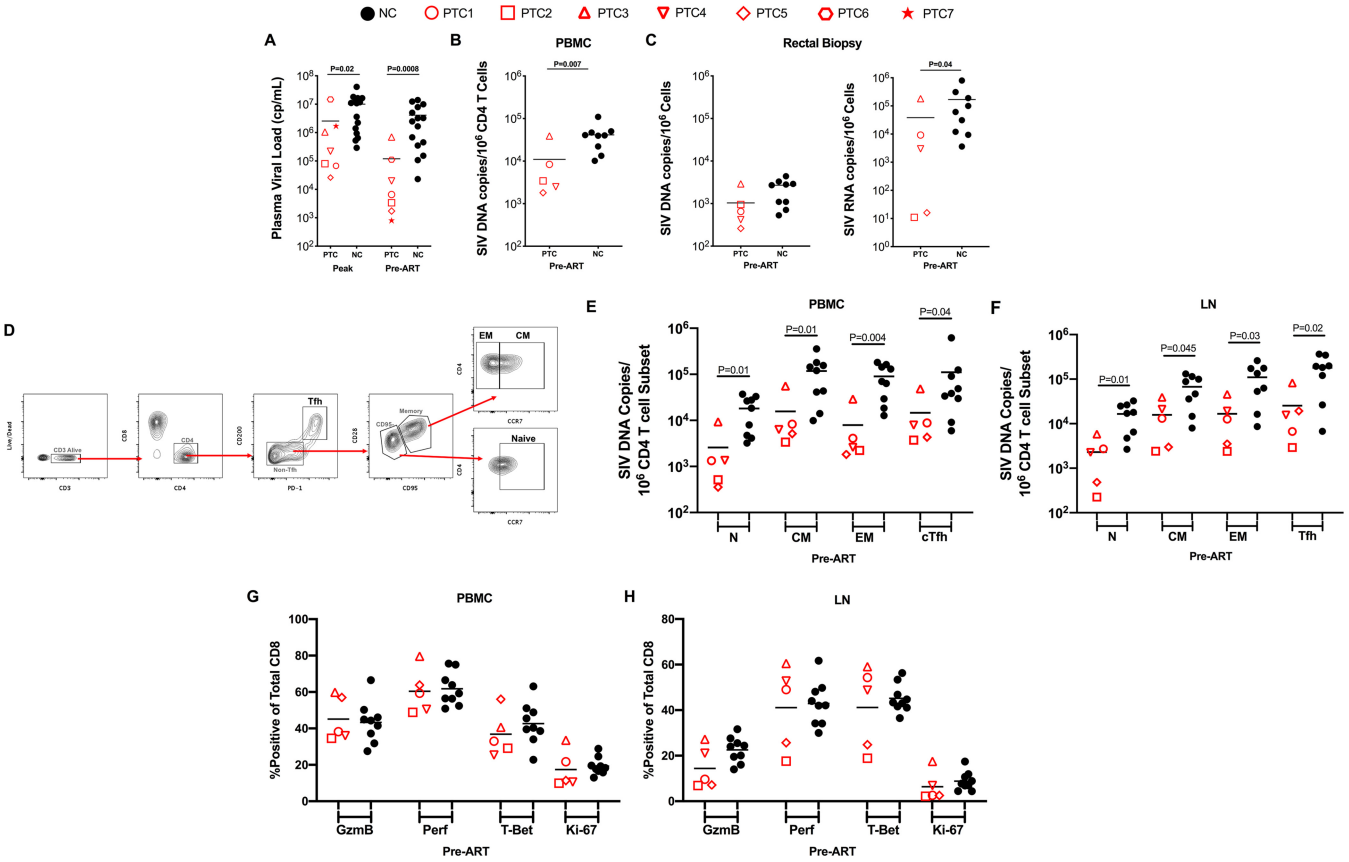

FIG 2 PTCs have reduced viral burden prior to ART initiation. (A) Plasma viral load levels at peak infection and pre-ART time points. (B) Total SIV DNA levels in purified blood CD4 T cells pre-ART. (C) Cell associated SIV DNA and RNA levels in total rectal biopsy samples pre-ART. (D) Gating strategy for CD4 T cell subsets from LN. (E) SIV DNA levels in sorted CD4 T cell subsets from peripheral blood (E) and lymph node (F) at a pre-ART time point. (G and H) Expression of CD8 T cell functional markers (GzmB, granzyme B; Perf, perforin) on total CD8 T cells in peripheral blood (G) and LN (H). Lines designate mean values.

NC distribution among the two regimens: (i) tenofovir (PMPA), emtricitabine (FTC), raltegravir, and ritonavir-boosted darunavir (5 PTC and 9 NC); or (ii) tenofovir (TDF), FTC, and dolutegravir (DTG) (2 PTC and 6 NC). Furthermore, at ATI, all PTCs and NCs reached plasma viremia below the limit of detection (<60 copies/ml) of our standard assay, confirming a comparable efficacy of the two treatments. Control of plasma viremia after ATI in PTCs was partial, with detectable plasma viremia (>60 copies/ml) in 6 out of 7 RMs (Fig. 1A). However, viral control was clearly superior compared to NCs, with more than a 3-log difference in the average plasma viremia among the two groups of RMs up to 8 months post-ATI (mean: 2.1 versus 5.9 $\log_{10}$ copies/ml; Fig. 1C).

RM PTCs had reduced SIV loads, but similar CD8 T cell responses, prior to ART initiation. Taking advantage of the availability of specimens collected at multiple phases of infection, we first investigated if animals that became PTCs had a reduced pathogenic SIV infection before initiation of ART compared to NCs. The levels of plasma viremia were significantly lower in PTCs than NCs both at peak (mean: 6.4 versus 7.0 $\log_{10}$ copies/ml, $P = 0.02$) and at chronic phase (mean: 5.1 versus 6.6 $\log_{10}$ copies/ml, $P = 0.0008$) of infection (Fig. 2A). Due to sample availability and timing of analyses, only 5 of the 7 identified PTCs and 9 of the 15 NCs (PTCs 1 to 5 and NCs 1 to 9) were included in subsequent analyses. Prior to ART initiation at week 8 postinfection, levels of total SIV DNA in peripheral blood CD4 T cells (mean: 10,991 versus 41,405 SIV DNA copies per 10^6 CD4 T cells, $P = 0.007$; Fig. 2B) and cell-associated SIV RNA in the colorectal tissue (mean: 38,445 versus 168,556 SIV RNA copies per 10^6 total cells, $P = 0.04$; Fig. 2C) were lower in PTCs compared to NCs, while levels of SIV DNA in colorectal tissue showed only a nonsignificant trend toward lower levels in PTCs (mean: 1,036 versus 2,171 SIV DNA

copies per 10^6 CD4 T cells, $P = 0.09$; Fig. 2C). To further investigate if the PTC status was associated with reduced infection of a specific CD4 T cell subset, we then purified naive ($CD28^+$ $CD95^-$ $CCR7^+$), central memory (T_{CM}; $CD95^+$ $CCR7^+$), effector memory (T_{EM}; $CD95^+$ $CCR7^-$), and T follicular helper (T_{FH}; PD-1^+ $CD200^{hi}$) CD4 T cell subsets from blood and LN. A representative staining with the detailed gating strategy for LN is shown in Fig. 2D. Of note, we previously showed that PD-1^+ $CD200^{hi}$ and PD-1^+ $CXCR5^+$ identify the same frequency of Tfh cells in the LN of SIV-infected RMs (20). In both peripheral blood (Fig. 2E) and LN (Fig. 2F), levels of total SIV DNA were significantly lower in PTCs compared to NCs for all measured CD4 T cell subsets ($P < 0.05$ for all comparisons). Thus, reduced levels of SIV replication and lower frequencies of infected cells in all CD4 T cell subsets prior to ART is a general feature distinguishing RM PTCs from NCs.

To address potential differences in CD8 responses between NCs and PTCs, we assessed cytolytic capacity and proliferation of total CD8 T cells prior to ART initiation in both peripheral blood and LN. Specifically, we analyzed *ex vivo* (without stimulation) levels of granzyme B, perforin, T-bet, and Ki-67 by flow cytometry on total CD8 T cells. Our analysis revealed no biologically important differences between NCs and PTCs in expression of these markers, indicating similar CD8 cytolytic potential and proliferative response within these animals despite different viral burdens pre-ART ($P > 0.05$ for all comparisons; Fig. 2G and H).

RM PTCs had reduced SIV-induced immunopathogenesis prior to ART initiation. We then investigated the main immunologic differences between RM PTCs and NCs before ART initiation. Consistent with reduced levels of SIV infection, and despite similar baseline (preinfection) levels, PTCs displayed significantly higher CD4 T cell counts (mean: 684 versus 451 CD4 T cells per μl blood, $P = 0.02$; Fig. 3A) and lower frequency of activated (HLA-DR^+ $CD38^+$) memory CD4 T cells (mean: 4.6% versus 8.4%, $P = 0.03$; Fig. 3B; Fig. S1A) than NCs in blood prior to starting ART. Consistently, the preinfection to pre-ART change for blood CD4 T cell counts (mean change $= -42$ for PTCs, $P = 0.55$; and mean change $= -253$ for NCs, $P < 0.001$) and % of HLA-DR^+ $CD38^+$ memory CD4 T cells (mean change $= -0.9\%$ for PTCs, $P = 0.56$; and mean change $= 4.2\%$ for NCs, $P = 0.004$) followed different patterns between the PTC and NC groups. A trend toward better maintenance of CD4 T cells, as assessed by frequency of $CD4^+$ cells in total $CD3^+$ cells, was also observed in LN (mean: 56% versus 44%, $P = 0.15$; Fig. 3C).

Recently, multiple studies have highlighted the loss of intestinal CD4 T cells, particularly those belonging to the Th17 subset, as a main cause of compromised mucosal integrity and systemic immune activation during HIV and SIV infection (21–26). Interestingly, our comparative analyses showed that the frequency of bulk intestinal CD4 T cells at preinfection and at initiation of ART were very similar between NCs and PTCs (Fig. 3D). We also found equivalent levels of memory CD4 T-cell activation in mucosal tissue (Fig. S1B). Th17 cells, defined as intestinal memory CD4 T cells expressing IL-17 after brief *in vitro* stimulation, were also present at comparable frequencies preinfection (Fig. 3E). However, after SIV infection, NCs experienced a considerably larger loss of Th17 cells than PTCs ($P = 0.007$; Fig. 3E), with reduction to 74% and 25% of their baseline level, respectively ($P = 0.001$; Fig. 3F). Representative staining before infection and before ART initiation is shown in Fig. 3G. Significantly higher maintenance of Th17 cells, despite equivalent loss of total CD4 T cells in the gut, is remarkably similar to the phenomenon observed when comparing nonpathogenic SIV infection of sooty mangabeys with pathogenic models of SIV infection in RMs (21). Of note, although limited to 5 PTCs and 9 NCs, receiver operating characteristic curve (ROC) analysis suggests that total SIV DNA content in peripheral blood CD4 T cells and frequency of Th17 cells in the gut were the two pre-ART markers most strongly associated with increased likelihood of developing a PTC status (Fig. S2A), with an area under the curve (AUC) of 0.93 for both predictors. The estimated AUC indicates a 93% probability that a PTC animal had a higher (or lower) predicted probability of PTC status than an NC animal for a random pair of animals with and without the outcome.

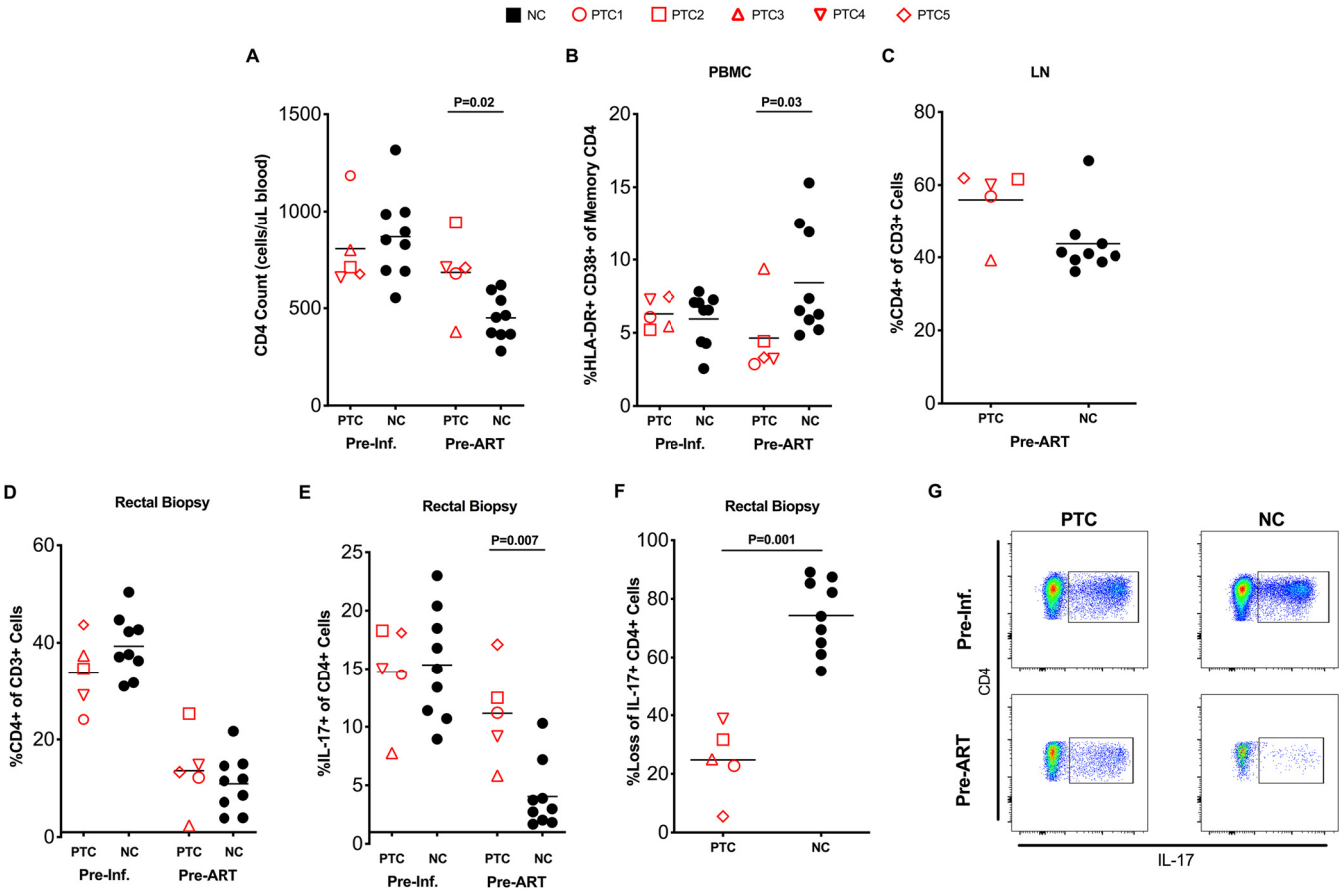

FIG 3 PTCs experience reduced immunopathogenesis prior to ART initiation. (A) CD4 counts in peripheral blood at preinfection and pre-ART time points. (B) CD4 T cell activation in peripheral blood preinfection and pre-ART as assessed by flow cytometry as HLA-DR$^+$ CD38$^+$ memory CD4 T cells. (C) CD4 frequency in lymph node pre-ART. (D) CD4 frequency in rectal biopsy samples preinfection and pre-ART. (E) Th17 frequency in rectal biopsy samples as assessed by flow cytometry as the frequency of memory CD4 T cells expressing IL-17 after a brief *in vitro* stimulation. (F) Levels of Th17 cells shown as the percentage of Th17 cells lost from the preinfection to pre-ART time points. Lines represent mean values. (G) Representative staining showing the identification of Th17 cells at preinfection and pre-ART time points.

Viral reservoir and immune dynamics of PTCs differ from NCs during ART. We then assessed the viral and immunological status of NCs and PTCs during ART, prior to ATI. First, we assessed the presence of residual viremia by using an ultrasensitive viral load assay with a limit of detection of 3 copies of SIVmac$_{239}$/ml of plasma (27). Consistent with their lower viral loads before ART, PTCs were significantly faster to suppress residual viremia while on ART compared to NCs, with 4 out of 5 animals (80%) at 75 days and 5 out of 5 (100%) at 200 days after ART initiation achieving a plasma viral load of $<$3 copies/ml, compared to 0 out of 9 (0%) and 3 out of 9 (33%) for NCs, respectively (day 75: $P = 0.002$; day 200: $P = 0.04$; Fig. 4A). While SIV DNA content declined in both PTCs and NCs during ART, PTCs continued to harbor lower levels of SIV DNA in CD4 T cells from peripheral blood both at a mid (mean: 2,608 versus 7,402 SIV DNA copies per 10^6 CD4 T cells, $P = 0.04$) and late ART (mean: 367 versus 1,596 SIV DNA copies per 10^6 CD4 T cells, $P = 0.004$) time point (Fig. 4B). The total SIV DNA content in peripheral blood CD4 T cells before ART interruption was the parameter with the strongest association with the development of a PTC status (AUC of 0.96; Fig. S2B). We further assessed levels of replication-competent, inducible SIV in LN CD4 T cells during ART using a quantitative viral outgrowth assay. PTCs harbored a significantly lower frequency of latently infected CD4 T cells compared to NCs (mean: 0.16 versus 4.46 infectious units per million; Fig. 4C). Since LN CD4 T cells expressing high levels of PD-1 have been identified as one of the main cellular targets for HIV/SIV infection and persistence, we then measured their frequency among our animals (28). Consistent

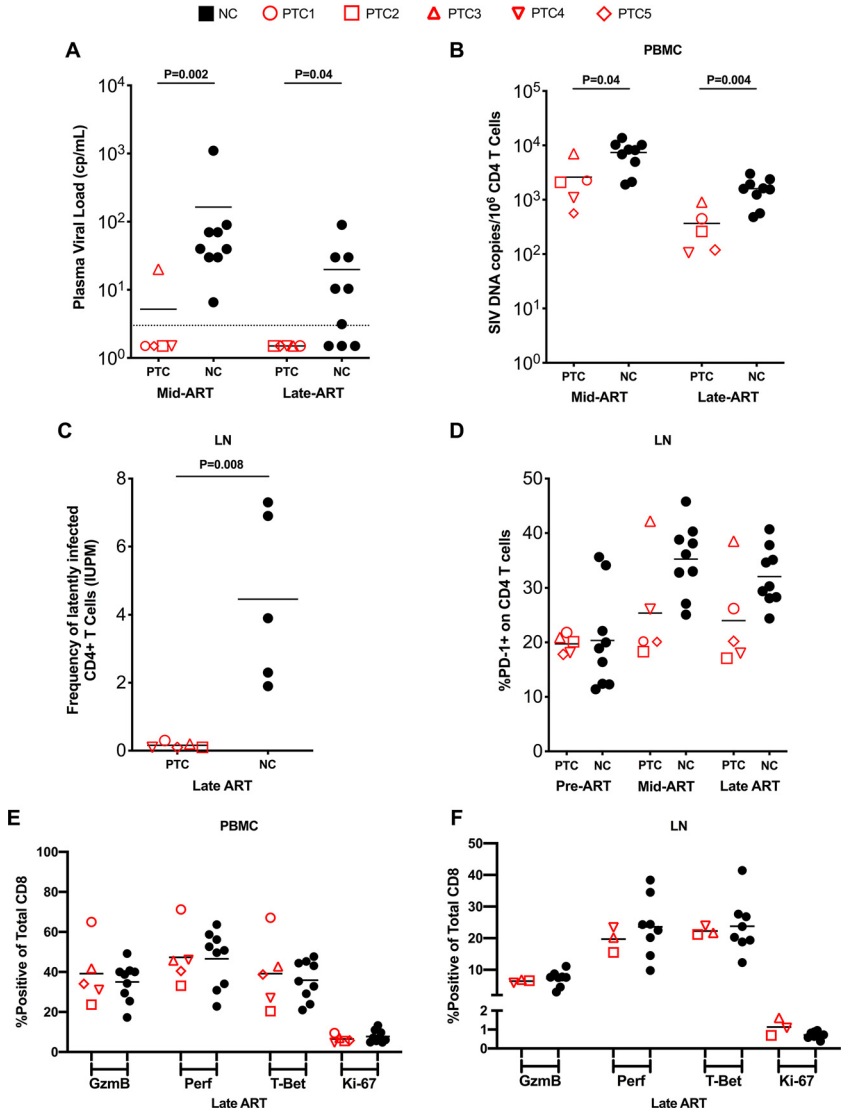

FIG 4 Reservoir and immune characteristics of PTCs and NCs on ART. (A) Viral load as determined by ultrasensitive assay (LOD = 3 copies/ml, dotted line) at mid-ART and late-ART. (B) SIV DNA levels in purified CD4 T cells from peripheral blood at mid-ART and late-ART. (C) Frequency of latently infected LN cells at late-ART, expressed as infectious units per million CD4 T cells, assessed by quantitative viral outgrowth assay. (D) Levels of PD-1 expression on CD4 T cells in LN at pre-ART, mid-ART, and late-ART. (E and F) Expression of CD8 T cell functional markers on total CD8 T cells in peripheral blood (E) and LN (F). Lines designate mean values.

with the lower level of replication-competent reservoir in LN, and despite similar levels at pre-ART, PTCs showed a trend toward lower levels of PD-1$^+$ CD4$^+$ T cells in LN throughout ART (Fig. 4D), providing further support for distinct reservoir environments within NCs and PTCs. However, as seen prior to ART, there was no difference in cytolytic capacity or proliferation of CD8 T cells between PTCs and NCs on ART in both peripheral blood and LN (Fig. 4E and F).

RM PTCs show preservation of immunological homeostasis during 8 months of ATI. Along with marked differences in viral rebound, we assessed immunological characteristics that distinguished the PTCs and NCs after ATI. After treatment interruption, RM PTCs maintained stable CD4 T cell levels in peripheral blood, while NCs experienced significant loss of CD4 T cells, as expected during normal disease progression (Fig. 5A). Notably, this immune preservation extended to mucosal tissues. Despite similar levels of total mucosal CD4 T cells prior to and throughout the duration of ART,

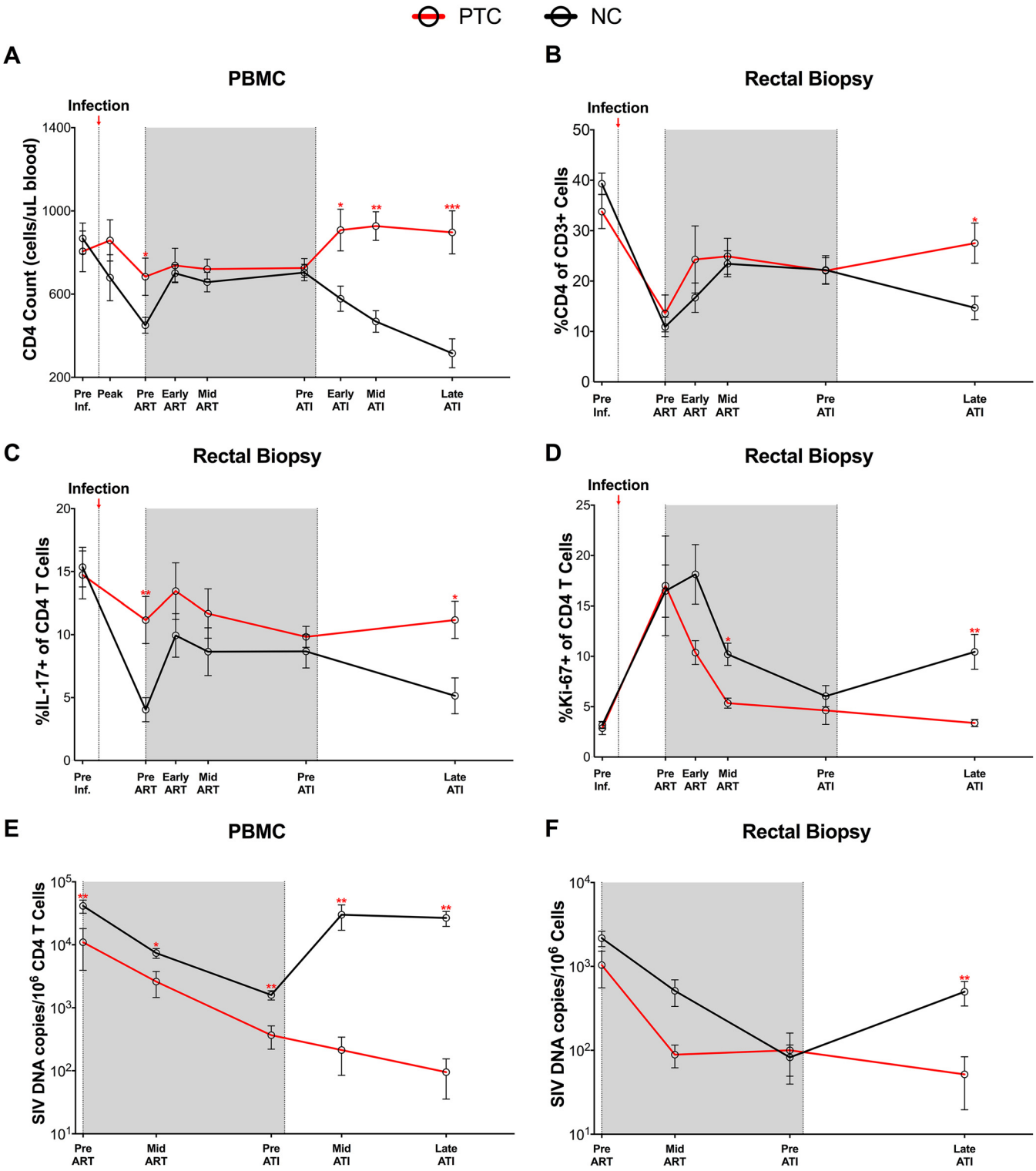

FIG 5 PTCs maintain viral control and preserve immune homeostasis during ATI. (A) Longitudinal CD4 counts in peripheral blood. (B to D) Longitudinal frequency of total CD4 T cells (B), Th17 cells (C), and proliferating CD4 T cells (D) in rectal biopsy samples. (E and F) Longitudinal SIV DNA levels in PBMC (E) and rectal biopsy samples (F). Data shown as means ± standard error of the mean (SEM). PTCs 1 to 5 and NCs 1 to 9 were included in this analysis. See the Materials and Methods for time point definitions. Shaded area designates period for which animals were on ART. *, $P < 0.05$; **, $P < 0.005$; ***, $P < 0.0005$.

PTCs had a significantly higher frequency of CD4 T cells after treatment interruption (mean: 27.5% versus 14.7% $CD4^+$ of $CD3^+$, $P = 0.03$; Fig. 5B). Furthermore, similar to the environment observed prior to ART, there was a continued maintenance of Th17 cells in PTCs but not NCs (mean: 11.2% versus 5.1% IL-17^+ of $CD4^+$, $P = 0.03$; Fig. 5C). Finally, we observed significantly lower levels of intestinal CD4 T cell proliferation in PTCs compared to NCs when using Ki-67, a marker for which expression has been associated with loss of function of mucosal T cells in SIV infection (mean: 3.4% versus 10.5% K_i-67^+ of $CD4^+$, $P = 0.004$; Fig. 5D) (24).

To follow up on the lower viral burden observed prior to and on ART, we assessed levels of cell-associated virus in peripheral blood CD4 T cells and in colorectal biopsy samples also following ATI. We found significantly lower levels of total SIV DNA in blood CD4 T cells in PTCs compared to NCs at multiple time points during the ATI (mid: 213 versus 29,976 copies SIV DNA per 10^6 CD4 T cells, $P = 0.002$; late: 95 versus 26,706 copies SIV DNA per 10^6 CD4 T cells, $P = 0.001$; Fig. 5E). Similarly, in colorectal tissue samples, despite having equivalent levels of SIV DNA at the time of ART interruption, PTCs had lower levels of total SIV DNA at a late-ATI time point (mean: 52 versus 499 copies SIV DNA per 10^6 total cells, $P = 0.002$; Fig. 5F). Remarkably, in both peripheral blood mononuclear cells (PBMC) and mucosal tissue, despite the absence of ART for more than 6 months and persistent plasma viremia in the majority of animals, PTCs experienced stable or even decreasing levels of SIV DNA. All together, these data highlight the ability of PTCs to maintain both immune homeostasis and viral control in the absence of ART, while NCs experience continued disease progression.

DISCUSSION

Achieving sustained control of HIV replication in the absence of ART is a critical goal for people living with HIV and the most important readout for currently tested HIV cure strategies. Unfortunately, no interventions have shown efficacy in achieving HIV remission after treatment interruption in humans. The identification of human PTCs, generally characterized by their ability to maintain plasma viral loads at less than 400 copies/ml for at least 6 months following ATI (5–12), offers an important opportunity to identify key mechanisms contributing to HIV remission and provide targets for future interventions. This study identifies 7 SIV-infected RM PTCs that exhibit robust control of viremia for an extended period after ATI and adds to the growing knowledge of the immunologic and virologic characteristics of individuals who maintain low viral load in the absence of ART.

The RM PTCs described in this study mirror much of what has been seen in cohorts of HIV-infected human PTCs. For up to 8 months post-ATI, at which point the study was terminated, RM PTCs maintained viral loads remarkably lower than the NCs and experienced decreased pathogenesis, with significantly higher CD4 counts and lower immune activation in blood. Thus, virologic control did result in clinically relevant immunologic benefits for the RM PTCs. This is important, since a functional cure needs not only to control viral replication but also to reconstitute and maintain a functional immune system. In addition, RM PTCs harbored lower levels of SIV DNA than NCs at all time points of infection. In particular, as observed in multiple human PTC cohorts, total SIV DNA content at the time of ART interruption was lower in RM PTCs than NCs (8, 11, 17, 29). While this assay largely measures defective viral DNA, it has been shown that human PTCs do not harbor a significantly different ratio of defective to intact HIV genomes compared to NCs (17). The lower levels of total SIV DNA pre-ATI in RM PTCs fits with what was seen in the SPARTAC study of acutely treated HIV-infected individuals, in which it was found that HIV DNA levels at ART cessation predicted time to viral rebound (30). Importantly, taking advantage of the RM model, we were able to extend our analysis to lymphoid tissue. In addition to the periphery, using a quantitative viral outgrowth assay we found lower levels of replication-competent virus in CD4 T cells of lymph nodes from RM PTCs compared to NCs, in agreement with our measures of total DNA content. Furthermore, in both LN and PBMC, we found lower levels of SIV DNA in naive, central memory, effector memory, and T follicular helper subsets of CD4 T cells,

suggesting that RM PTCs have an overall lower viral burden that is not limited to a particular anatomic location or differentiation subset. In lymphoid tissues, PD-1$^+$ CD4 T cells have been previously described as a main contributor to HIV/SIV persistence due to their enrichment for HIV content and the ability of PD-1, once engaged, to inhibit HIV production and limit HIV reactivation (28, 31, 32). RM PTCs showed lower levels of PD-1$^+$ CD4 T cells in LN throughout ART, which could indicate an environment less favorable to viral persistence. Interestingly, during ATI, the low levels of SIV DNA remained stable in both peripheral blood and colorectal tissues, with some animals showing a decrease after ART interruption, despite the presence of detectable viremia in most animals. This suggests that, after ART withdrawal, PTCs are capable of clearing virally infected cells at a rate at least equivalent to the rate of new cell infection in the presence of viremia.

Identification of a PTC population within an SIV model allowed for tissue access and assessment of populations previously undescribed in human PTCs. Importantly, we found that the continued maintenance of CD4 T cells during ATI described in peripheral blood of human PTCs extends to both lymphoid and mucosal sites in RM PTCs. Furthermore, we were able to assess mucosal Th17 cells throughout primary infection, ART suppression, and treatment interruption. Th17 cells are among the first cells to be infected after HIV transmission (33), harbor high levels of HIV DNA (34–36), and are preferentially depleted following HIV and SIV infection, and this loss is known to be a main driver of mucosal barrier breakdown, systemic immune activation, and disease progression (21–26, 37). Before initiation of ART, mucosal CD4 T cells were similarly depleted in RM PTCs and NCs; however, PTCs selectively maintained higher frequencies of Th17 cells than NCs. This phenotype is remarkably similar to what is observed in the nonpathogenic SIV infection in the natural host sooty mangabey (SM), which, following SIV infection, have a significant depletion of CD4$^+$ T cells from mucosal sites but maintain normal levels of Th17 cells and do not experience systemic immune activation equivalent to the pathogenic infection of RMs (38). Our findings in RM PTCs, which experienced significantly less Th17 loss and peripheral immune activation compared to NCs, continue to support these described relationships between Th17 preservation, chronic immune activation, and disease outcome. Early ART initiation in HIV-infected individuals has also been shown to preserve Th17 cells and mucosal integrity, and is also associated with higher occurrence of posttreatment control (15, 39, 40). Synthesis of these findings in humans, in conjunction with our findings in RMs, suggests a model in which the early initiation of ART limits viral exposure and preserves mucosal immune integrity, both of which are likely contributors to the development of posttreatment control in a subset of individuals. Furthermore, the demonstrated maintenance of CD4 T cell populations in both lymph node and mucosal tissue in RM PTCs in the absence of ART strongly suggests that even partial control of viremia can prevent immune dysfunction.

There are several caveats associated with this study. First, analyses were performed *post hoc* on RMs selected from studies not directly intended to assess posttreatment control. Animals in those studies initiated ART 8 weeks after SIV infection thus, although very unlikely based on many studies of SIVmac$_{239}$ infection in RMs, we cannot fully rule out the possibility that these PTCs may have progressed to spontaneous control of plasma viremia in the absence of ART (8). Furthermore, since some animals received immune-based interventions in addition to ART, for those we cannot discriminate between the relative contribution of ART or immune-based intervention in inducing the PTC phenotype. However, it is important to note that those interventions were shown to have no significant impact on viral rebound, that PTC incidence was not increased in treated animals, and that our NCs also included animals receiving the same immune-based interventions (Table S1) (41, 42). While RM PTCs did have a lower viral burden at ART initiation compared to controls, this alone is not enough to indicate future control without ART. Cases of spontaneous controller RM infected with SIVmac$_{239}$ have been reported, but are typically associated with favorable MHC class I alleles Mamu-B*08 and B*17, similar to human elite controllers with HLA-B*57 and HLA-B*27 alleles (18, 19). In

analyses of Mamu-B*08- and B*17-negative RMs infected with the same $SIVmac_{239}$ virus and who never initiate ART, natural control is rarely observed by our group or others, even in animals with low set point viral loads (data not shown). We did observe a higher frequency of Mamu-A*01 in the PTC group compared to NC, raising the possibility that Mamu-A*01 may predispose a subset of RMs to posttreatment control but may not be strong enough to induce spontaneous control. Importantly, while we were unable to assess SIV-specific CD8 T cells, we did not find differences between RM PTCs and NCs with regard to cytolytic capacity or proliferative response of total CD8 T cells, neither prior to nor after ART. This is in agreement with reports that HIV-specific CD8 responses are generally weak in human PTCs compared to spontaneous controllers and viremic individuals (6, 43, 44). It is likely, however, that the decreased systemic presence of SIV in the PTC animals prior to starting ART critically contributed to their capacity to control viremia at ATI. Data on human PTCs vary by cohort, with most showing equivalent set point viral loads to NCs but some showing decreased viral load at ART initiation in PTCs (5, 6, 8). It has also been demonstrated in humans that HIV DNA content at the time of starting ART is lower in PTCs than NCs (8). Our data on RM PTCs support the notion that lower HIV levels in both tissue and blood contribute to control of viremia after ATI. Unfortunately, the retroactive nature of our analysis prevents any further mechanistic characterization of the PTC phenomenon described here. Further studies in RM could be designed to specifically address outstanding mechanistic questions of posttreatment control, particularly with regard to the importance of the timing of ART initiation and the role of CD8 T cells in this viral control.

In summary, our data identify 7 SIV-infected RMs characterized as PTCs due to their ability to maintain viral control after cessation of ART. Our RM PTCs exhibit virologic and immunologic characteristics largely similar to those previously reported in cohorts of HIV-infected PTCs, and we extend this analysis into previously unexplored periods of infection and anatomical sites. Importantly, our data highlight the benefits of limiting immune activation, immune damage, and the size of the reservoir early in HIV/SIV infection, all most achievable by early ART initiation, to promote potential viral control. It may be valuable to tailor early stages of intervention trials toward individuals who initiated ART early or who harbor small reservoirs, as they are likely best positioned to experience a positive outcome. Lastly, this report highlights the importance of including nonintervention control arms in all studies in both the SIV and HIV fields, to allow for best analysis of intervention-specific impact on viral control in the absence of ART.

MATERIALS AND METHODS

Animals, SIV infection, and antiretroviral therapy. Twenty-two Indian rhesus macaques (RMs) all housed at the Yerkes National Primate Research Center (YNPRC) in Atlanta, GA, were selected for this study. All RMs were *Mamu*-B*08^{-} and *Mamu*-B*17^{-}; A*01 status for all animals is listed in Table S1. All RMs were infected intravenously with $SIVmac_{239}$ (provided by Koen Van Rompay, U.C. Davis) at the dose designated in Table S1. Approximately 8 weeks postinfection, all RMs initiated daily antiretroviral therapy. Fourteen animals were on a regimen composed of tenofovir (PMPA; 20 to 25 mg/kg/d, subcutaneous [s.c.]), emtricitabine (FTC; 30 to 50 mg/kg/d, s.c.), raltegravir (100 to 150 mg/bid, oral), darunavir (400 to 700 mg/bid, oral), and ritonavir (50 mg/bid, oral). Eight animals were on a regimen composed of dolutegravir (DTG; 2.5 mg/kg/d, s.c.), tenofovir disoproxil fumarate (TDF; 5.1 mg/kg/d, s.c.), and emtricitabine (FTC; 40 mg/kg/d, s.c.). Animals received daily ART for up to 60 weeks. All animals reached viral loads below the limit of detection (60 copies/ml) for multiple time points before undergoing analytic treatment interruption (ATI), at which point animals were followed for up to 8 months until necropsy.

In addition to ART, RM designated "IL-21 treated" in Table S1 were treated with recombinant IL-21–IgFc at the beginning and at the end of ART and at the beginning of ATI (41). Animals designated "aCTLA-4/aPD-1 treated" in Table S1 received bi-specific αCTLA-4/αPD-1 IgG1 over 4 weeks starting 6 weeks prior to ATI (42).

Study approval. All animal experimentation was conducted following guidelines set forth by the Animal Welfare Act and by the NIH's Guide for the Care and Use of Laboratory Animals, 8th edition. All studies were reviewed and approved by Emory's Institutional Animal Care and Use Committee (IACUC; permit numbers 3000065, 2003297, 2003470, 201700665, and 2001973) and animal care facilities at YNPRC are accredited by the U.S. Department of Agriculture (USDA) and the Association for Assessment and Accreditation of Laboratory Animal Care (AAALAC) International. Proper steps were taken to minimize animal suffering and all procedures were conducted under anesthesia with follow-up pain management as needed.

Experimental time points. For consistency across groups, time points were defined as the following: preinfection (15 to 21 days preinfection); peak infection (D14 postinfection [p.i.]); early infection (D28 to 42 p.i.); pre-ART/ART initiation (D56 to 60 p.i.); early ART (D84 to 102 p.i.); mid ART (D110 to 140 p.i); late ART (D197 to 256 p.i.); pre-ATI (13 to 15 days pre-ATI); early ATI (D27 to 28 post-ATI); mid ATI (D59 to 60 post-ATI); and late ATI (D180 to 240 post-ATI).

Sample collection and processing. Peripheral blood, lymph node, and rectal biopsy sample collections were conducted throughout the study and were processed as previously described (45).

Flow cytometry. Fourteen parameter flow cytometry was performed on collected tissues according to previously optimized standard procedures using anti-human antibodies that have been shown to be cross-reactive with RMs. The following antibodies were used: (from BD Biosciences) anti-CD3–APC–Cy7 (clone SP34-2), anti-CD95–PE–Cy5 (clone DX2), anti-CD28-PE-594 (clone CD28.2), anti-Ki-67-Alexa Fluor 700 (clone B56), anti-CD8-PE-CF-594 (clone RPA-T8), anti-CCR7-PE-Cy7 (clone 3D12), anti-HLA-DR-PerCp-Cy5.5 (clone G46-6); anti-IL-17-Alexa Fluor 488 (clone eBio64DEC17, eBioscience); (from Biolegend) anti-CD4-BV421 (clone OKT4), anti-CD4-BV605 (clone OKT4), anti-PD1-PE (clone EH12.2H7), anti-PD1-BV421 (clone EH12.2H7), anti-T-Bet-PE (clone eBio4B10), anti-CD200-PE (clone OX104); (from Invitrogen) anti-CD8-Qdot705 (clone 3B5), anti-GzmB-PE-TR (clone GB11), Aqua LIVE/DEAD amine dye AmCyan; anti-CD38-FITC (clone AT-1; STEMCELL Technologies); and anti-Perforin-FITC (clone-Pf344; MABTECH). Flow cytometric acquisition was performed on at least 100,000 $CD3^+$ T cells on a BD LSR II flow cytometer driven by BD FACSDiva software and analysis of the acquired data was performed using FlowJo software.

Th17 analysis. Th17 cells in rectal biopsy samples were determined as previously described (24). Briefly, isolated cells were stimulated for 4 h with phorbol myristate acetate (PMA) and A23187 in the presence of BD GolgiStop, stained for surface markers, permeabilized, and stained intracellularly for cytokines. Th17 levels were determined as the percentage of memory CD4 T cells that produced IL-17.

Plasma viral load. Levels of SIV RNA copies in plasma were determined by real-time reverse transcriptase quantitative PCR (qRT-PCR) as previously described with a limit of detection (LOD) of 60 copies/ml, with values below the LOD imputed as half of the LOD (46). Ultrasensitive measurements were performed by ultracentrifugation at the described time points on ART as previously described (27).

Cell-associated SIV DNA and RNA measurements. SIV DNA and RNA levels in rectal biopsy samples, as well as SIV DNA in peripheral CD4 T cells, were assessed quantitatively by qRT-PCR assays as previously described (41). For analysis of SIV DNA content in CD4 T cell subsets, isolated cells from peripheral blood and lymph node were sorted on a FACS AriaII (BD Biosciences) into the following CD4 T cell subsets: naive ($CD28^+$ $CD95^-$ $CCR7^+$), central memory (T_{CM}; $CD95^+$ $CCR7^+$), effector memory (T_{EM}; $CD95^+$ $CCR7^-$), and T follicular helper (T_{FH}; PD-1^+ $CD200^{hi}$) cells. Sorting strategy is shown in Fig. 2D. SIV DNA levels were then assessed on sorted populations as previously described (41).

Quantification of replication-competent virus in CD4 T cells from lymph node. CD4 T cells were purified from cryopreserved lymph node samples and assessed for levels of replication-competent SIV as previously described (41). Briefly, cells were cocultured with CEMx174 cells (NIH AIDS Reagent Program) in serial dilutions for 25 days, with analysis at days 9, 16, and 25. Positive wells were determined based on flow cytometric analysis of SIV-Gag p27 expression and SIV-GAG viral RNA detection by qPCR, and frequencies of infected cells were determined by maximum likelihood method (47) and expressed as infectious units per million CD4 T cells.

Statistical analysis. Statistical tests were all two-sided and P values of ≤ 0.05 were considered to be statistically significant for each comparison. Data plotted as longitudinal grouped analysis are displayed as means $\pm$ SEM unless otherwise indicated. Comparisons of parameters between noncontrollers and posttreatment controllers were calculated using Mann-Whitney U tests. Analyses were conducted using GraphPad Prism 8.3. Analysis of mean change for CD4 T cell count and % HLA-DR^+ $CD38^+$ of blood memory CD4 was done by repeated-measures analyses using a mixed-effects model via the SAS MIXED Procedure (version 9.4; SAS Institute, Cary, NC), providing separate estimates of the means by time on study and study group (48). Two approaches were used to evaluate PB SIV DNA and Th17 frequency as potential markers or predictors of PTC status. First, the risk of PTC status was modeled as a function of PB SIV DNA (and separately using Th17 frequency) by using logistic regression (outcome = PTC or NC). Second, marker performance was summarized with classification performance measures, such as sensitivity, specificity, the receiver operating characteristic curves (ROC), and the area under the curve (AUC). The AUC for each marker can be interpreted as the probability that a PTC animal had a higher (or lower) predicted probability of PTC status than an NC animal, for random pairs with and without the outcome.

SUPPLEMENTAL MATERIAL

Supplemental material is available online only.

SUPPLEMENTAL FILE 1, PDF file, 3.3 MB.

ACKNOWLEDGMENTS

We thank Sherrie Jean, Stephanie Ehnert, Christopher Souder, and all veterinary and animal care staff at Yerkes. We also would like to acknowledge the Emory Flow Cytometry Core (Barbara Cervasi and Kiran Gill) and the Emory CFAR Virology Core (Thomas Vanderford) for their assistance with flow cytometry and viral load measurements.

This work was supported by the NIAID, NIH, under award numbers R01AI116379 and R01AI11034 to M. Paiardini, award P30AI050409 to the Center for AIDS Research at

Emory University, and ORIP/OD award P51OD011132 to the Yerkes National Primate Research Center. Viral load assays were performed in the Quantitative Molecular Diagnostics Core of the AIDS and Cancer Virus Program of the Frederick National Laboratory for Cancer Research and supported in part with federal funds from the Frederick National Laboratory for Cancer Research under contract number 75N91019D00024. The content of this publication does not necessarily reflect the views or policies of the Department of Health and Human Services, nor does mention of trade names, commercial products, or organizations imply endorsement by the U.S. Government.

REFERENCES

1. Bhaskaran K, CASCADE Collaboration, Hamouda O, Sannes M, Boufassa F, Johnson AM, Lambert PC, Porter K. 2008. Changes in the risk of death after HIV seroconversion compared with mortality in the general population. JAMA 300:51–59. https://doi.org/10.1001/jama.300.1.51.
2. The Antiretroviral Therapy Cohort Collaboration. 2008. Life expectancy of individuals on combination antiretroviral therapy in high-income countries: a collaborative analysis of 14 cohort studies. Lancet 372:293–299. https://doi.org/10.1016/S0140-6736(08)61113-7.
3. Wong JK, Hezareh M, Günthard HF, Havlir DV, Ignacio CC, Spina CA, Richman DD. 1997. Recovery of replication-competent HIV despite prolonged suppression of plasma viremia. Science 278:1291–1295. https://doi.org/10.1126/science.278.5341.1291.
4. Chun T-W, Carruth L, Finzi D, Shen X, DiGiuseppe JA, Taylor H, Hermankova M, Chadwick K, Margolick J, Quinn TC, Kuo Y-H, Brookmeyer R, Zeiger MA, Barditch-Crovo P, Siliciano RF. 1997. Quantification of latent tissue reservoirs and total body viral load in HIV-1 infection. Nature 387:183–188. https://doi.org/10.1038/387183a0.
5. Namazi G, Fajnzylber JM, Aga E, Bosch RJ, Acosta EP, Sharaf R, Hartogensis W, Jacobson JM, Connick E, Volberding P, Skiest D, Margolis D, Sneller MC, Little SJ, Gianella S, Smith DM, Kuritzkes DR, Gulick RM, Mellors JW, Mehraj V, Gandhi RT, Mitsuyasu R, Schooley RT, Henry K, Tebas P, Deeks SG, Chun T-W, Collier AC, Routy J-P, Hecht FM, Walker BD, Li JZ. 2018. The control of HIV after antiretroviral medication pause (CHAMP) study: posttreatment controllers identified from 14 clinical studies. J Infect Dis 218:1954–1963. https://doi.org/10.1093/infdis/jiy479.
6. Sáez-Cirión A, ANRS VISCONTI Study Group, Bacchus C, Hocqueloux L, Avettand-Fenoel V, Girault I, Lecuroux C, Potard V, Versmisse P, Melard A, Prazuck T, Descours B, Guergnon J, Viard J-P, Boufassa F, Lambotte O, Goujard C, Meyer L, Costagliola D, Venet A, Pancino G, Autran B, Rouzioux C. 2013. Post-treatment HIV-1 controllers with a long-term virological remission after the interruption of early initiated antiretroviral therapy ANRS VISCONTI study. PLoS Pathog 9:e1003211. https://doi.org/10.1371/journal.ppat.1003211.
7. Sneller MC, Justement JS, Gittens KR, Petrone ME, Clarridge KE, Proschan MA, Kwan R, Shi V, Blazkova J, Refsland EW, Morris DE, Cohen KW, McElrath MJ, Xu R, Egan MA, Eldridge JH, Benko E, Kovacs C, Moir S, Chun T-W, Fauci AS. 2017. A randomized controlled safety/efficacy trial of therapeutic vaccination in HIV-infected individuals who initiated antiretroviral therapy early in infection. Sci Transl Med 9:eaan8848. https://doi.org/10.1126/scitranslmed.aan8848.
8. Martin GE, Gossez M, Williams JP, Stöhr W, Meyerowitz J, Leitman EM, Goulder P, Porter K, Fidler S, Frater J. 2017. Post-treatment control or treated controllers? Viral remission in treated and untreated primary HIV infection. AIDS 31:477–484. https://doi.org/10.1097/QAD.0000000000001382.
9. Fidler S, Olson AD, Bucher HC, Fox J, Thornhill J, Morrison C, Muga R, Phillips A, Frater J, Porter K. 2017. Virological blips and predictors of post treatment viral control after stopping ART started in primary HIV infection. J Acquir Immune Defic Syndr 74:126–133. https://doi.org/10.1097/QAI.0000000000001220.
10. Lodi S, Meyer L, Kelleher AD, Rosinska M, Ghosn J, Sannes M, Porter K. 2012. Immunovirologic control 24 months after interruption of antiretroviral therapy initiated close to HIV seroconversion. Arch Intern Med 172:1252–1255. https://doi.org/10.1001/archinternmed.2012.2719.
11. Van Gulck E, Bracke L, Heyndrickx L, Coppens S, Atkinson D, Merlin C, Pasternak A, Florence E, Vanham G. 2012. Immune and viral correlates of "secondary viral control" after treatment interruption in chronically HIV-1 infected patients. PLoS One 7:e37792. https://doi.org/10.1371/journal.pone.0037792.
12. Calin R, Hamimi C, Lambert-Niclot S, Carcelain G, Bellet J, Assoumou L, Tubiana R, Calvez V, Dudoit Y, Costagliola D, Autran B, Katlama C. 2016. Treatment interruption in chronically HIV-infected patients with an ultralow HIV reservoir. AIDS 30:761–769. https://doi.org/10.1097/QAD.0000000000000987.
13. Samri A, ANRS VISCONTI study group, Bacchus-Souffan C, Hocqueloux L, Avettand-Fenoel V, Descours B, Theodorou I, Larsen M, Saez-Cirion A, Rouzioux C, Autran B. 2016. Polyfunctional HIV-specific T cells in Post-Treatment Controllers. AIDS 30:2299–2302. https://doi.org/10.1097/QAD.0000000000001195.
14. Migueles SA, Connors M. 2010. Long-term nonprogressive disease among untreated HIV-infected individuals. JAMA 304:194. https://doi.org/10.1001/jama.2010.925.
15. Etemad B, Esmaeilzadeh E, Li JZ. 2019. Learning from the exceptions: HIV remission in post-treatment controllers. Front Immunol 10:1749. https://doi.org/10.3389/fimmu.2019.01749.
16. Assoumou L, Weiss L, Piketty C, Burgard M, Melard A, Girard P-M, Rouzioux C, Costagliola D. 2015. A low HIV-DNA level in peripheral blood mononuclear cells at antiretroviral treatment interruption predicts a higher probability of maintaining viral control. AIDS 29:2003–2007. https://doi.org/10.1097/QAD.0000000000000734.
17. Sharaf R, Lee GQ, Sun X, Etemad B, Aboukhater LM, Hu Z, Brumme ZL, Aga E, Bosch RJ, Wen Y, Namazi G, Gao C, Acosta EP, Gandhi RT, Jacobson JM, Skiest D, Margolis DM, Mitsuyasu R, Volberding P, Connick E, Kuritzkes DR, Lederman MM, Yu XG, Lichterfeld M, Li JZ. 2018. HIV-1 proviral landscapes distinguish posttreatment controllers from noncontrollers. J Clin Invest 128:4074–4085. https://doi.org/10.1172/JCI120549.
18. Loffredo JT, Friedrich TC, León EJ, Stephany JJ, Rodrigues DS, Spencer SP, Bean AT, Beal DR, Burwitz BJ, Rudersdorf RA, Wallace LT, Piaskowski SM, May GE, Sidney J, Gostick E, Wilson NA, Price DA, Kallas EG, Piontkivska H, Hughes AL, Sette A, Watkins DI. 2007. CD8+ T cells from SIV elite controller macaques recognize Mamu-B*08-bound epitopes and select for widespread viral variation. PLoS One 2:e1152. https://doi.org/10.1371/journal.pone.0001152.
19. Yant LJ, Friedrich TC, Johnson RC, May GE, Maness NJ, Enz AM, Lifson JD, O'Connor DH, Carrington M, Watkins DI. 2006. The high-frequency major histocompatibility complex class I allele Mamu-B*17 is associated with control of simian immunodeficiency virus SIVmac239 replication. JVI 80:5074–5077. https://doi.org/10.1128/JVI.80.10.5074-5077.2006.
20. Pino M, Paganini S, Deleage C, Padhan K, Harper JL, King CT, Micci L, Cervasi B, Mudd JC, Gill KP, Jean SM, Easley K, Silvestri G, Estes JD, Petrovas C, Lederman MM, Paiardini M. 2019. Fingolimod retains cytolytic T cells and limits T follicular helper cell infection in lymphoid sites of SIV persistence. PLoS Pathog 15:e1008081. https://doi.org/10.1371/journal.ppat.1008081.
21. Brenchley JM, Paiardini M, Knox KS, Asher AI, Cervasi B, Asher TE, Scheinberg P, Price DA, Hage CA, Kholi LM, Khoruts A, Frank I, Else J, Schacker T, Silvestri G, Douek DC. 2008. Differential Th17 CD4 T-cell depletion in pathogenic and nonpathogenic lentiviral infections. Blood 112:2826–2835. https://doi.org/10.1182/blood-2008-05-159301.
22. Cecchinato V, Trindade CJ, Laurence A, Heraud JM, Brenchley JM, Ferrari MG, Zaffiri L, Tryniszewska E, Tsai WP, Vaccari M, Parks RW, Venzon D, Douek DC, O'Shea JJ, Franchini G. 2008. Altered balance between Th17 and Th1 cells at mucosal sites predicts AIDS progression in simian immunodeficiency virus-infected macaques. Mucosal Immunol 1:279–288. https://doi.org/10.1038/mi.2008.14.

23. Micci L, Cervasi B, Ende ZS, Iriele RI, Reyes-Aviles E, Vinton C, Else J, Silvestri G, Ansari AA, Villinger F, Pahwa S, Estes JD, Brenchley JM, Paiardini M. 2012. Paucity of IL-21-producing CD4$^+$ T cells is associated with Th17 cell depletion in SIV infection of rhesus macaques. Blood 120:3925–3935. https://doi.org/10.1182/blood-2012-04-420240.
24. Ryan ES, Micci L, Fromentin R, Paganini S, McGary CS, Easley K, Chomont N, Paiardini M. 2016. Loss of function of intestinal IL-17 and IL-22 producing cells contributes to inflammation and viral persistence in SIV-infected rhesus macaques. PLoS Pathog 12:e1005412. https://doi.org/10.1371/journal.ppat.1005412.
25. Pallikkuth S, Micci L, Ende ZS, Iriele RI, Cervasi B, Lawson B, McGary CS, Rogers KA, Else JG, Silvestri G, Easley K, Estes JD, Villinger F, Pahwa S, Paiardini M. 2013. Maintenance of intestinal Th17 cells and reduced microbial translocation in SIV-infected rhesus macaques treated with interleukin (IL)-21. PLoS Pathog 9:e1003471. https://doi.org/10.1371/journal.ppat.1003471.
26. Klatt NR, Estes JD, Sun X, Ortiz AM, Barber JS, Harris LD, Cervasi B, Yokomizo LK, Pan L, Vinton CL, Tabb B, Canary LA, Dang Q, Hirsch VM, Alter G, Belkaid Y, Lifson JD, Silvestri G, Milner JD, Paiardini M, Haddad EK, Brenchley JM. 2012. Loss of mucosal CD103+ DCs and IL-17+ and IL-22+ lymphocytes is associated with mucosal damage in SIV infection. Mucosal Immunol 5:646–657. https://doi.org/10.1038/mi.2012.38.
27. Del Prete GQ, Shoemaker R, Oswald K, Lara A, Trubey CM, Fast R, Schneider DK, Kiser R, Coalter V, Wiles A, Wiles R, Freemire B, Keele BF, Estes JD, Quiñones OA, Smedley J, Macallister R, Sanchez RI, Wai JS, Tan CM, Alvord WG, Hazuda DJ, Piatak M, Lifson JD. 2014. Effect of suberoylanilide hydroxamic acid (SAHA) administration on the residual virus pool in a model of combination antiretroviral therapy-mediated suppression in SIVmac239-infected Indian rhesus macaques. Antimicrob Agents Chemother 58:6790–6806. https://doi.org/10.1128/AAC.03746-14.
28. Banga R, Procopio FA, Noto A, Pollakis G, Cavassini M, Ohmiti K, Corpataux J-M, de Leval L, Pantaleo G, Perreau M. 2016. PD-1+ and follicular helper T cells are responsible for persistent HIV-1 transcription in treated aviremic individuals. Nat Med 22:754–761. https://doi.org/10.1038/nm.4113.
29. Goujard C, the ANRS CO6 PRIMO Study Group, Girault I, Rouzioux C, Lécuroux C, Deveau C, Chaix M-L, Jacomet C, Talamali A, Delfraissy J-F, Venet A, Meyer L, Sinet M. 2012. HIV-1 control after transient antiretroviral treatment initiated in primary infection: role of patient characteristics and effect of therapy. Antivir Ther 17:1001–1009. https://doi.org/10.3851/IMP2273.
30. Williams JP, on behalf of the SPARTAC trial investigators, Hurst J, Stöhr W, Robinson N, Brown H, Fisher M, Kinloch S, Cooper D, Schechter M, Tambussi G, Fidler S, Carrington M, Babiker A, Weber J, Koelsch KK, Kelleher AD, Phillips RE, Frater J. 2014. HIV-1 DNA predicts disease progression and post-treatment virological control. Elife 3:e03821. https://doi.org/10.7554/eLife.03821.
31. Fromentin R, Bakeman W, Lawani MB, Khoury G, Hartogensis W, DaFonseca S, Killian M, Epling L, Hoh R, Sinclair E, Hecht FM, Bacchetti P, Deeks SG, Lewin SR, Sékaly R-P, Chomont N. 2016. CD4+ T cells expressing PD-1, TIGIT and LAG-3 contribute to HIV persistence during ART. PLoS Pathog 12:e1005761. https://doi.org/10.1371/journal.ppat.1005761.
32. Fromentin R, DaFonseca S, Costiniuk CT, El-Far M, Procopio FA, Hecht FM, Hoh R, Deeks SG, Hazuda DJ, Lewin SR, Routy JP, Sékaly RP, Chomont N. 2019. PD-1 blockade potentiates HIV latency reversal ex vivo in CD4 + T cells from ART-suppressed individuals. Nat Commun 10:814. https://doi.org/10.1038/s41467-019-08798-7.
33. Stieh DJ, Matias E, Xu H, Fought AJ, Blanchard JL, Marx PA, Veazey RS, Hope TJ. 2016. Th17 cells are preferentially infected very early after vaginal transmission of SIV in macaques. Cell Host Microbe 19:529–540. https://doi.org/10.1016/j.chom.2016.03.005.
34. Wacleche VS, Goulet J-P, Gosselin A, Monteiro P, Soudeyns H, Fromentin R, Jenabian M-A, Vartanian S, Deeks SG, Chomont N, Routy J-P, Ancuta P. 2016. New insights into the heterogeneity of Th17 subsets contributing to HIV-1 persistence during antiretroviral therapy. Retrovirology 13:59. https://doi.org/10.1186/s12977-016-0293-6.
35. Gosselin A, Wiche Salinas TR, Planas D, Wacleche VS, Zhang Y, Fromentin R, Chomont N, Cohen ÉA, Shacklett B, Mehraj V, Ghali MP, Routy J-P, Ancuta P. 2017. HIV persists in CCR6+CD4+ T cells from colon and blood during antiretroviral therapy. AIDS 31:35–48. https://doi.org/10.1097/QAD.0000000000001309.
36. Khoury G, Anderson JL, Fromentin R, Hartogenesis W, Smith MZ, Bacchetti P, Hecht FM, Chomont N, Cameron PU, Deeks SG, Lewin SR. 2016. Persistence of integrated HIV DNA in CXCR3 + CCR6 + memory CD4+ T cells in HIV-infected individuals on antiretroviral therapy. AIDS 30:1511–1520. https://doi.org/10.1097/QAD.0000000000001029.
37. Macal M, Sankaran S, Chun T-W, Reay E, Flamm J, Prindiville TJ, Dandekar S. 2008. Effective CD4+ T-cell restoration in gut-associated lymphoid tissue of HIV-infected patients is associated with enhanced Th17 cells and polyfunctional HIV-specific T-cell responses. Mucosal Immunol 1:475–488. https://doi.org/10.1038/mi.2008.35.
38. Gordon SN, Klatt NR, Bosinger SE, Brenchley JM, Milush JM, Engram JC, Dunham RM, Paiardini M, Klucking S, Danesh A, Strobert EA, Apetrei C, Pandrea IV, Kelvin D, Douek DC, Staprans SI, Sodora DL, Silvestri G. 2007. Severe depletion of mucosal CD4 + T cells in AIDS-free simian immunodeficiency virus-infected sooty mangabeys. J Immunol 179:3026–3034. https://doi.org/10.4049/jimmunol.179.5.3026.
39. Kök A, Hocqueloux L, Hocini H, Carrière M, Lefrou L, Guguin A, Tisserand P, Bonnabau H, Avettand-Fenoel V, Prazuck T, Katsahian S, Gaulard P, Thiébaut R, Lévy Y, Hüe S. 2015. Early initiation of combined antiretroviral therapy preserves immune function in the gut of HIV-infected patients. Mucosal Immunol 8:127–140. https://doi.org/10.1038/mi.2014.50.
40. Schuetz A, Deleage C, Sereti I, Rerknimitr R, Phanuphak N, Phuang-Ngern Y, Estes JD, Sandler NG, Sukhumvittaya S, Marovich M, Jongrakthaitae S, Akapirat S, Fletscher JLK, Kroon E, Dewar R, Trichavaroj R, Chomchey N, Douek DC, O'Connell RJ, Ngauy V, Robb ML, Phanuphak P, Michael NL, Excler J-L, Kim JH, de Souza MS, Ananworanich J, RV254/SEARCH 010 and RV304/SEARCH 013 Study Groups. 2014. Initiation of ART during early acute HIV infection preserves mucosal Th17 function and reverses HIV-related immune activation. PLoS Pathog 10:e1004543. https://doi.org/10.1371/journal.ppat.1004543.
41. Micci L, Ryan ES, Fromentin R, Bosinger SE, Harper JL, He T, Paganini S, Easley KA, Chahroudi A, Benne C, Gumber S, McGary CS, Rogers KA, Deleage C, Lucero C, Byrareddy SN, Apetrei C, Estes JD, Lifson JD, Piatak M, Chomont N, Villinger F, Silvestri G, Brenchley JM, Paiardini M. 2015. Interleukin-21 combined with ART reduces inflammation and viral reservoir in SIV-infected macaques. J Clin Invest 125:4497–4513. https://doi.org/10.1172/JCI81400.
42. Harper J, Gordon S, Chan CN, Wang H, Lindemuth E, Galardi C, Falcinelli SD, Raines SLM, Read JL, Nguyen K, McGary CS, Nekorchuk M, Busman-Sahay K, Schawalder J, King C, Pino M, Micci L, Cervasi B, Jean S, Sanderson A, Johns B, Koblansky AA, Amrine-Madsen H, Lifson J, Margolis DM, Silvestri G, Bar KJ, Favre D, Estes JD, Paiardini M. 2020. CTLA-4 and PD-1 dual blockade induces SIV reactivation without control of rebound after antiretroviral therapy interruption. Nat Med 26:519–528. https://doi.org/10.1038/s41591-020-0782-y.
43. Frange P, Faye A, Avettand-Fenoël V, Bellaton E, Descamps D, Angin M, David A, Caillat-Zucman S, Peytavin G, Dollfus C, Le Chenadec J, Warszawski J, Rouzioux C, Sáez-Cirión A. 2016. HIV-1 virological remission lasting more than 12 years after interruption of early antiretroviral therapy in a perinatally infected teenager enrolled in the French ANRS EPF-CO10 paediatric cohort: a case report. Lancet HIV 3:e49–e54. https://doi.org/10.1016/S2352-3018(15)00232-5.
44. Salgado M, Rabi SA, O'Connell KA, Buckheit Iii RW, Bailey JR, Chaudhry AA, Breaud AR, Marzinke MA, Clarke W, Margolick JB, Siliciano RF, Blankson JN. 2011. Prolonged control of replication-competent dual-tropic human immunodeficiency virus-1 following cessation of highly active antiretroviral therapy. Retrovirology 8:97. https://doi.org/10.1186/1742-4690-8-97.
45. McGary CS, Deleage C, Harper J, Micci L, Ribeiro SP, Paganini S, Kuri-Cervantes L, Benne C, Ryan ES, Balderas R, Jean S, Easley K, Marconi V, Silvestri G, Estes JD, Sekaly R-P, Paiardini M. 2017. CTLA-4$^+$PD-1$^-$ Memory CD4$^+$ T cells critically contribute to viral persistence in antiretroviral therapy-suppressed, SIV-infected rhesus macaques. Immunity 47:776–788.e5. https://doi.org/10.1016/j.immuni.2017.09.018.
46. Hofmann-Lehmann R, Swenerton RK, Liska V, Leutenegger CM, Lutz H, McClure HM, Ruprecht RM. 2000. Sensitive and robust one-tube real-time reverse transcriptase-polymerase chain reaction to quantify SIV RNA load: comparison of one- versus two-enzyme systems. AIDS Res Hum Retroviruses 16:1247–1257. https://doi.org/10.1089/08892220050117014.
47. Myers LE, McQuay LJ, Hollinger FB. 1994. Dilution assay statistics. J Clin Microbiol 32:732–739. https://doi.org/10.1128/JCM.32.3.732-739.1994.
48. Diggle P, Liang K, Zeger S. 1994. Analysis of longitudinal data. Clarendon Press, Oxford, United Kingdom.